

# Radiation Transport in Tokamak Edge Plasmas

*H.A. Scott, M.L. Adams*

This article was submitted to 16<sup>th</sup> International Conference on  
Spectral Line Shapes (ICSLS), Berkeley, CA, June 3-7, 2002

**September 30, 2002**

*U.S. Department of Energy*

Lawrence  
Livermore  
National  
Laboratory

## DISCLAIMER

This document was prepared as an account of work sponsored by an agency of the United States Government. Neither the United States Government nor the University of California nor any of their employees, makes any warranty, express or implied, or assumes any legal liability or responsibility for the accuracy, completeness, or usefulness of any information, apparatus, product, or process disclosed, or represents that its use would not infringe privately owned rights. Reference herein to any specific commercial product, process, or service by trade name, trademark, manufacturer, or otherwise, does not necessarily constitute or imply its endorsement, recommendation, or favoring by the United States Government or the University of California. The views and opinions of authors expressed herein do not necessarily state or reflect those of the United States Government or the University of California, and shall not be used for advertising or product endorsement purposes.

This is a preprint of a paper intended for publication in a journal or proceedings. Since changes may be made before publication, this preprint is made available with the understanding that it will not be cited or reproduced without the permission of the author.

This report has been reproduced directly from the best available copy.

Available electronically at <http://www.doc.gov/bridge>

Available for a processing fee to U.S. Department of Energy  
And its contractors in paper from  
U.S. Department of Energy  
Office of Scientific and Technical Information  
P.O. Box 62  
Oak Ridge, TN 37831-0062  
Telephone: (865) 576-8401  
Facsimile: (865) 576-5728  
E-mail: [reports@adonis.osti.gov](mailto:reports@adonis.osti.gov)

Available for the sale to the public from  
U.S. Department of Commerce  
National Technical Information Service  
5285 Port Royal Road  
Springfield, VA 22161  
Telephone: (800) 553-6847  
Facsimile: (703) 605-6900  
E-mail: [orders@ntis.fedworld.gov](mailto:orders@ntis.fedworld.gov)  
Online ordering: <http://www.ntis.gov/ordering.htm>

OR

Lawrence Livermore National Laboratory  
Technical Information Department's Digital Library  
<http://www.llnl.gov/tid/Library.html>

# Radiation Transport in Tokamak Edge Plasmas

H. A. Scott, M. L. Adams\*

*University of California, Lawrence Livermore National Laboratory  
P.O. Box 808, Livermore, CA 94551, USA*

*\*Department of Nuclear Engineering, Massachusetts Institute of Technology  
NW16-230, 167 Albany St., Cambridge, MA 02139, USA*

**Abstract.** Plasmas in edge regions of tokamaks can be very optically thick to hydrogen lines. Strong line radiation introduces a non-local coupling between different regions of the plasma and can significantly affect the ionization and energy balance. These effects can be very important, but they are not included in current edge plasma simulations. We report here on progress in self-consistently including the effects of a magnetic field, line radiation and plasma transport in modeling tokamak edge plasmas.

## INTRODUCTION

High-density low-temperature plasmas with electron temperatures of order 1 eV and electron densities greater than  $10^{15} \text{ cm}^{-3}$  have been observed in the edge regions of the Alcator C-Mod [1] and D-III-D tokamaks [2]. At these temperatures and densities, the mean free path of a Lyman- $\alpha$  photon is less than 0.1 cm and the plasma can be very optically thick to line radiation. Optically thick Lyman lines have been confirmed experimentally [3]. However, simulations of these edge plasmas currently treat line radiation solely as an energy loss mechanism, assuming that the radiation can escape freely. Since the radiation field includes a significant amount of energy, a more realistic treatment of line radiation is needed for edge plasma simulations.

Wan, *et al* [4] addressed these issues for the first time in the context of a radiative divertor design for ITER. They used temperature and ion density profiles obtained with the UEDGE code [5] and recalculated the ionization balance and radiation flux to the divertor plate including line transfer effects. The results showed that the ionization balance changed significantly and the radiation flux decreased dramatically. Excitation by (primarily) Lyman- $\alpha$  line radiation allowed ionization to occur at much lower temperatures than otherwise predicted. These results were only suggestive, since the simulations were not self-consistent - changes in the ionization balance and radiative energy loss rate could not affect the ion and energy transport. Knoll saw similarly dramatic changes in self-consistent ITER-scale divertor simulations under the assumption that all Lyman- $\alpha$  radiation was trapped [6,7].

Our current research program is aimed at investigating the effects of radiation transport in these low temperature edge plasmas and providing computational tools for analyzing and simulating these plasmas. This paper is intended as both a brief description and a status report of the program to date.

For the plasma conditions considered here, which include magnetic fields of several Tesla, Stark and Doppler broadening and Zeeman splitting are of similar magnitudes for the lowest lines in the Lyman and Balmer series and must all be included in calculating line profiles. We calculate line profiles with the code TOTAL [8], which has been extended to include magnetic field effects. Line radiation transport is done with the code CRETIN [9], using profiles generated by TOTAL for the local conditions at each position in the edge plasma. This combined capability places an emphasis on robustness and computational efficiency in the line profile calculation. However, it allows for a consistent investigation of the interplay between the line profile, atomic kinetics and radiation transport, including an evaluation of the accuracy of less costly approximations. We demonstrate the use of the combined code with a sample calculation using conditions appropriate to Alcator C-Mod.

The following section discusses line profiles in magnetized plasmas, which are critical components in these investigations. The line profiles are important to the spatial and frequency distribution of the radiation field, which in turn influences the spatial variation of the excited-state populations and ionization balance, which ultimately affects the transport of (non-radiative) energy. Section 3 describes the use of magnetic line profiles in a line radiation transport code. While this is a useful and necessary step towards the desired simulation capability, it does not address the issue of adding radiation effects to an edge plasma simulation code. Section 4 discusses one possible avenue towards this goal and quantifies some optical depth effects. The paper concludes with a brief discussion of the next few steps in the research program.

## MAGNETIC LINE PROFILES

In this section we describe the incorporation of magnetic effects into the line shape code TOTAL. The intent here is to highlight the salient points. More details are available in a companion paper [10] and a comprehensive discussion is given in Adams, *et al* [11]. We describe first the formalism used in TOTAL, then the modifications required in the plasma average and atomic Hamiltonian for the inclusion of an external magnetic field.

### TOTAL Line Shape Formalism

TOTAL employs an electron collision operator formulated within the framework of a binary collision relaxation theory, plus a quasi-static electric ion microfield. The spectral line shape calculation considers only electric dipole transitions between bound states. Following standard line broadening theory, the line shape  $\phi(\omega)$  is calculated as the Fourier transform of the time correlation function of the dipole operator, averaged over all atomic and plasma states:

$$\begin{aligned} \phi(\omega) &= \int P(E) \phi(E, \omega) dE \\ &= \int P(E) \frac{1}{\pi} \operatorname{Re} \int_0^{\infty} \langle\langle \alpha \beta | \mathbf{d} e^{-\frac{i}{\hbar}(L_E - i\Gamma)t} \rho_i \mathbf{d} | \alpha' \beta' \rangle\rangle e^{i\omega t} dt dE \end{aligned} \quad (1)$$

where  $P(E)$  is the quasi-static electric ion microfield distribution function,  $\Gamma$  is the electron collision operator,  $\rho_i$  is the initial density matrix of the atomic system and  $|\alpha\beta\rangle\rangle$  represents the atomic state in Liouville space.  $L_E$  is the Liouville operator pertaining to the Hamiltonian  $H$  for a particular ionic field  $E$

$$H = H_a - \mathbf{E} \cdot \mathbf{d} \quad (2)$$

where  $H_a$  is the atomic Hamiltonian, and  $\mathbf{d}$  is the dipole operator. Matrix elements of the Liouville operator, i.e. energy levels and electric dipole matrix elements, are obtained from atomic structure calculations.

Following Calisti, *et al* [8], the computational approach centers around solving the complex eigenvalue problem for a fixed ionic field and then averaging over possible ionic fields. For a given ionic field  $E$ , the eigenvalues are easily obtained in the basis where  $L_E - i\Gamma$  is diagonal, resulting in

$$\phi(E_j, \omega) = \sum_k \frac{c_{1k}(\omega - x_k(E_j)) + c_{2k}y_k(E_j)}{(\omega - x_k(E_j))^2 + y_k(E_j)^2} \quad (3)$$

The line profile is then simply obtained as the sum of the components  $\phi(E_j, \omega)$ , weighted by the microfield distribution function. This approach has proved to be quite efficient, being limited primarily by the speed of the required eigenvalue calculations.

## Magnetic Field Modifications

The plasma average consists of two parts: the electron collision operator, which is calculated within the framework of binary collision relaxation theory, and the quasi-static electric ion microfield. An external magnetic field introduces a preferential axis into the system that destroys the arbitrary orientation of the electric dipole operator. It can also potentially alter the dynamical properties of the plasma [11], but we do not address that issue in here.

The quasi-static ion microfield model assumes that the emitting atom is surrounded by a spherically symmetric plasma. The electric dipole moment can be chosen to point in an arbitrary direction, while the ion microfield distribution must be a function only of ionic field strength. With the introduction of a preferential axis, the spherical symmetry is broken and the integration over the microfield distribution becomes anisotropic:

$$\int dE P(E) dE \rightarrow \int dE_{\parallel} P_{\parallel}(E_{\parallel}) \int dE_{\perp} P_{\perp}(E_{\perp}) \quad (4)$$

where the subscripts refer to the direction of the electric field relative to the magnetic field. The plasma average must now include an average over electric field directions relative to the magnetic field. This modification increases computational time by introducing a double integration, as well as tripling the number of non-zero electric dipole matrix elements that enter the complex eigenvalue problem. We assume that the microfield itself remains unchanged by the introduction of a magnetic field. A discussion of this point is included in [11].

The external magnetic field also introduces additional terms into the Hamiltonian. We include here only the paramagnetic term, which produces the Zeeman effect:

$$H = H_a - \mathbf{E} \cdot \mathbf{d} - \mu_B \mathbf{B} \cdot \left[ \mathbf{J} + (g_s - 1) \mathbf{S} \right] \quad (5)$$

for a state with quantum numbers  $\mathbf{J}$  and  $\mathbf{S}$ , where  $\mu_B$  is the Bohr magneton, and  $g_s$  is the electron gyromagnetic ratio. The additional (magnetic dipole) matrix element is evaluated by an atomic structure code in a similar manner to the electric dipole matrix element.

The positions of the Zeeman components in the resulting line profiles depend on the magnetic field strength, while the intensities of the Zeeman components vary with the direction of observation relative to the magnetic field. The line profile observed at an angle  $\beta$  relative to the magnetic field is given by

$$\phi(\omega, \beta) = \cos^2(\beta)\phi_{\parallel}(\omega) + \sin^2(\beta)\phi_{\perp}(\omega). \quad (6)$$

where the subscripts here refer to the observation direction relative to the magnetic field.

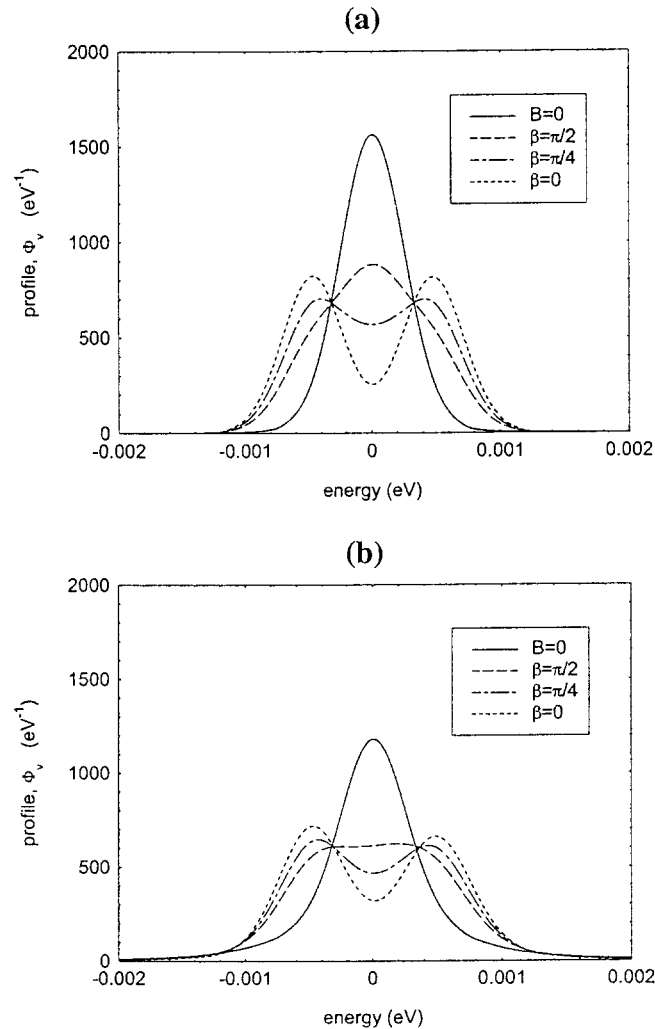


**FIGURE 1.** Line profiles for H Lyman- $\alpha$  at  $T_e=T_i=1$  eV with (a)  $n_e=10^{15}$   $\text{cm}^{-3}$ , (b)  $n_e=10^{16}$   $\text{cm}^{-3}$ . The energy scale here is relative to the position of the unbroadened transition. The solid curve is for  $B=0$  while the other curves are for  $B=8$  T for three different angles of observation  $\beta$ , measured relative to the magnetic field direction.

## Hydrogen Lyman- $\alpha$ and Balmer- $\alpha$ Profiles

Figure 1 shows the emission profiles for hydrogen Lyman- $\alpha$  in the presence of an 8T magnetic field for plasma temperatures of 1 eV and electron densities of  $10^{15}$  and  $10^{16}$   $\text{cm}^{-3}$ . For no magnetic field ( $B=0$ ), the line shape is the usual Voigt profile. While the magnetic field significantly affects the spectral line shape, the characteristic Lorentz triplet is not apparent. This is due to thermal broadening, which at  $T_i=1$  eV is comparable to the Zeeman splitting. Figure 2 shows the same profiles with  $T_i=.001$  eV, effectively removing thermal broadening. The Lorentz triplet now becomes visible (for  $\beta \neq 0$ ), as well as fine structure present in the individual peaks. Stark broadening remains evident, particularly at the higher electron density in Figure 2b. Note that Figure 2a uses a logarithmic scale.

Figure 3 shows the emission profiles for hydrogen Balmer- $\alpha$  for plasma temperatures of 1 eV and electron densities of  $10^{14}$  and  $10^{16}$   $\text{cm}^{-3}$ . Doppler broadening is less important for this lower transition energy, so Zeeman splitting is the dominant feature at low densities, while Stark broadening dominates at higher densities.

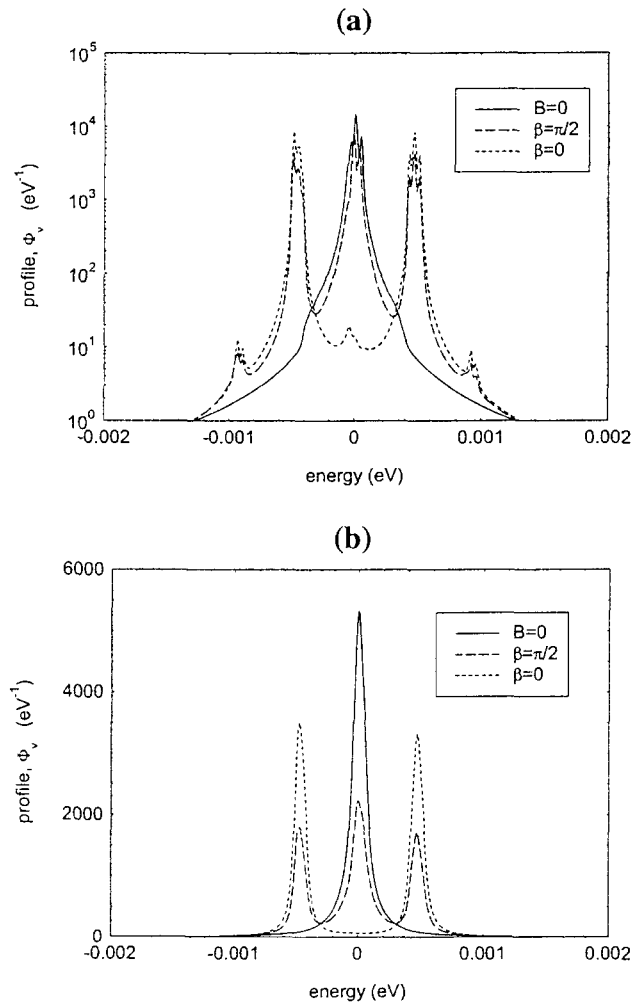
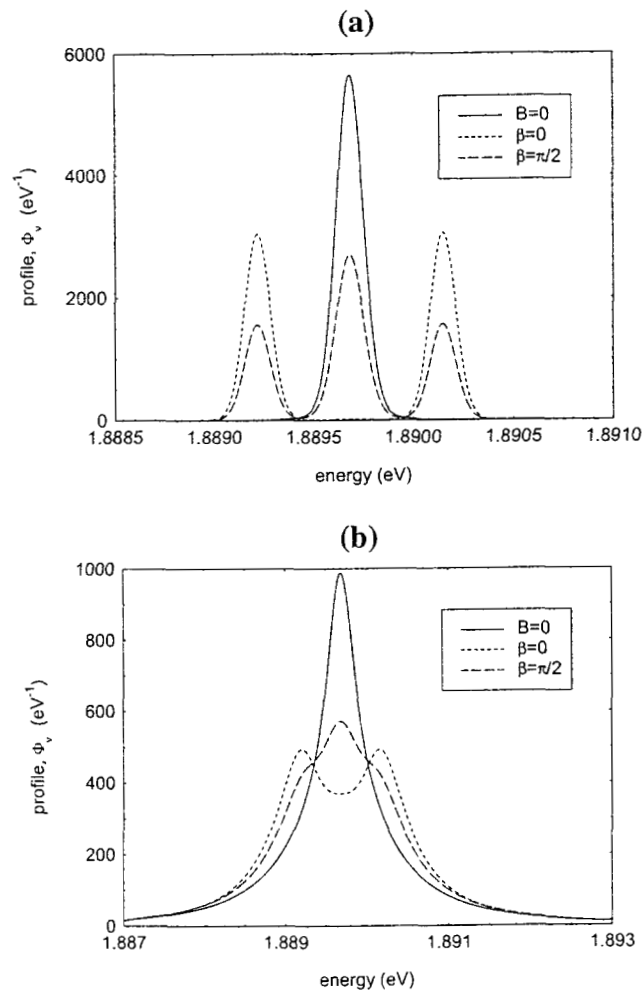


FIGURE 2. Same as Figure 1 with  $T_i=.001$  eV, for two angles of observation.

## MAGNETIC LINE RADIATION TRANSPORT

The modified TOTAL code has been fully integrated into the code CRETIN [9], which solves the equations of non-local thermodynamic equilibrium atomic kinetics with line radiation transport. As an example, we consider a one-dimensional plasma slab with conditions appropriate to Alcator C-Mod. The plasma has a thickness 5 cm and consists of hydrogen with atomic and electron number density both set to  $10^{14}$   $\text{cm}^{-3}$ , temperature of 1 eV, and magnetic field of 8T. Figures 4-6 show the results of a line transfer calculation using line profiles calculated for four different magnetic cases. The reference case (solid line) assumes no magnetic field. The next two cases assume that the magnetic field is in the plane of the slab (perpendicular to the direction of observation) or oriented normal to the slab, with line profiles varying with photon direction. The final case uses a direction-independent line profile, obtained by averaging the perpendicular and parallel line profiles.



**FIGURE 3.** Line profiles for H Balmer- $\alpha$  with  $T_e=T_i=1$  eV and (a)  $n_e=10^{14} \text{ cm}^{-3}$ , (b)  $n_e=10^{16} \text{ cm}^{-3}$ . The solid curve is for  $B=0$  while the other curves are for  $B=8$  T for two different angles of observation  $\beta$ , measured relative to the magnetic field direction.

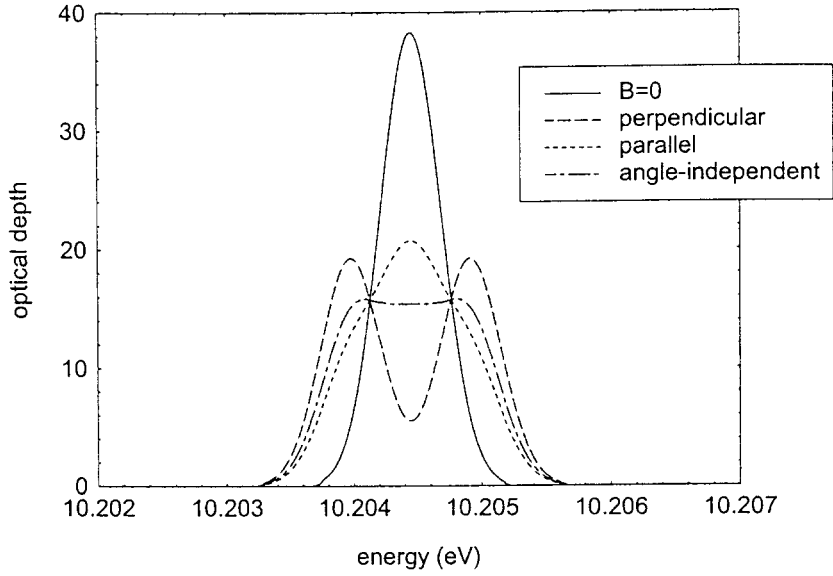


**FIGURE 4.** Optical depth for hydrogen Lyman- $\alpha$  as a function of energy for the 5 cm slab with  $n_e=10^{14} \text{ cm}^{-3}$  and  $T_e=T_i=1 \text{ eV}$ , measured normal to the slab surface. The solid curve is for  $B=0$  while the other curves are for  $B=8 \text{ T}$ . The dashed curve was calculated using line profiles for a magnetic field in the plane of the slab (perpendicular to the final direction of observation, which is normal to the slab surface). The dotted curve was calculated using a line profile for a magnetic field normal to the slab surface. The dot-dashed curve was calculated using a line profile that was the average of the perpendicular and parallel profiles regardless of the actual angle relative to the magnetic field.

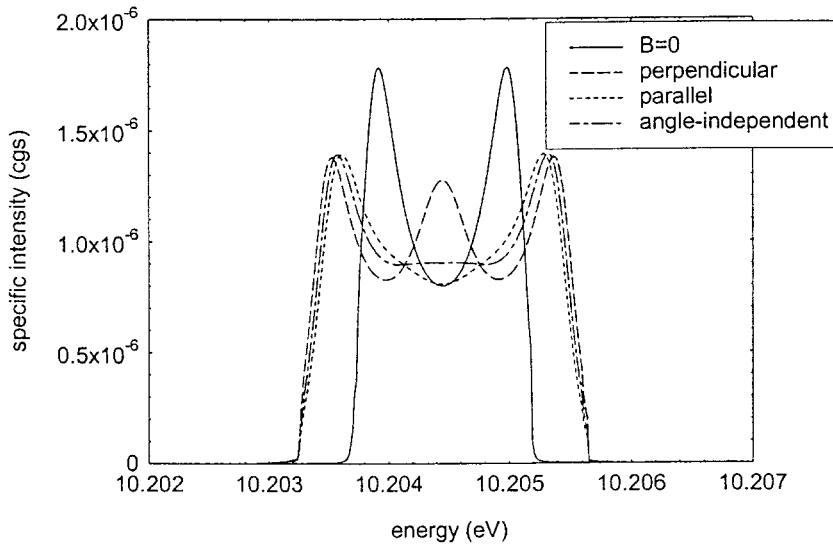


**FIGURE 5.** Specific intensity exiting normal to the slab surface, as a function of energy for the same cases as in Figure 4.

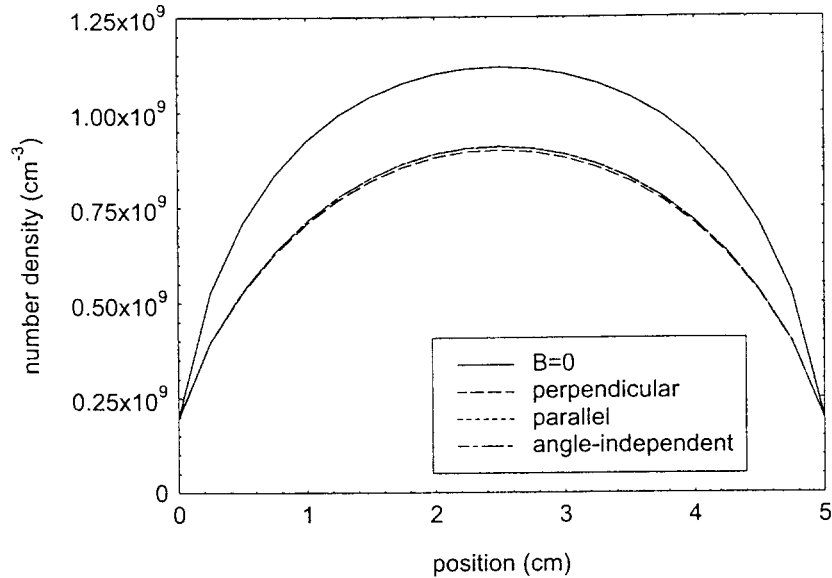


**FIGURE 6.** Upper state population for hydrogen Lyman- $\alpha$  as a function of position for the same cases as in Figure 4. The three curves with  $B=8$  T very nearly overlap.

Figure 4 shows the optical depth across the slab in a direction normal to the slab surface. This quantity depends only on the line absorption profile in this single direction and the (essentially) uniform distribution of ground state populations throughout the slab. Although the optical depth varies with direction (and magnetic field orientation), the maximum of this quantity across the line profile is a commonly used measure for quantifying line radiation effects. Broadening due to Zeeman splitting is evident and the peak optical depth has decreased by approximately a factor of two.

Figure 5 shows the radiation spectrum emerging from the plasma normal to the slab surface. The  $B=0$  case shows a strong inversion at line center, characteristic of an optically thick line. The parallel and perpendicular cases exhibit distinct spectral shapes, reflecting the magnetic field orientation. The total (integrated) radiation emitted increased by about 30% with the magnetic field present.

The effects of the radiation on the plasma are quite insensitive to the magnetic field orientation. This is demonstrated in Figure 6, which shows the upper state population density as a function of position. The magnitude of this quantity is much larger than the thermal value and is almost completely due to the effects of trapped line radiation. The value decreases towards the boundaries where radiation can escape more freely. The decreased trapping due to magnetic broadening results in a lower excited state population. Since this effect depends on the angle-integrated radiation intensity, it is insensitive to magnetic field orientation. This agrees with the results of Novikov, *et al* [12] in their investigation of magnetic field effects in radiation transfer through hydrogen plasmas.

## INTEGRATION INTO EDGE PLASMA CODES

The result that an angle-independent treatment is sufficient for calculating plasma effects is significant, since that should simplify the process of integrating radiation effects into an edge plasma code. In this section we discuss one possible approach towards including radiation effects, based on a generalization of the collisional-radiative model of Stotler, Post and Reiter (SPR) [13].

### SPR Collisional-Radiative Model

The plasma description generally used in an edge plasma code treats neutral hydrogen as a single species. Excited state distributions are not treated explicitly but become important at low temperatures and should be included in some manner. The approach of SPR uses a collisional-radiative model and assumes that the excited states are in equilibrium on plasma transport timescales. The excited states can then be expressed as functions of the ground state and ionized state. In this approach, the plasma transport deals explicitly with ground states and ionized states. The effects of excited state distributions enter through modified ionization and recombination coefficients. These coefficients are functions of temperature and electron density only, and are tabulated for use within the edge plasma code.

The excited state distributions affect the energy balance as well. Each ionization (recombination) results in an average gain (loss) of energy to the system of amount  $E_Z$  ( $E_R$ ). These quantities differ slightly from the ionization energy of 13.6 eV because of the finite width of the electron distribution function as well as excited state effects, and the differences between these values and 13.6 eV are the tabulated quantities, defined by

$$\delta E_Z = E_Z - 13.6 \text{ eV}, \quad \delta E_R = 13.6 \text{ eV} - E_R. \quad (7)$$

### Generalization of SPR Approach

The SPR coefficients depend only on temperature and electron density. Optically thick line radiation introduces a spatial dependence as well, through the variation of the radiation field. As a first approximation, we assume that we can parameterize the coefficients by optical depth. This is equivalent to an escape factor treatment of line transfer and should be valid for simple geometries, but will need to be checked by more detailed calculations for complex cases.

As a further simplification, we assume that the line profile does not change dramatically across the region of interest so that the neutral column density is proportional to the optical depth. An equivalent parameterization is then the effective distance to boundary  $R$ , defined by

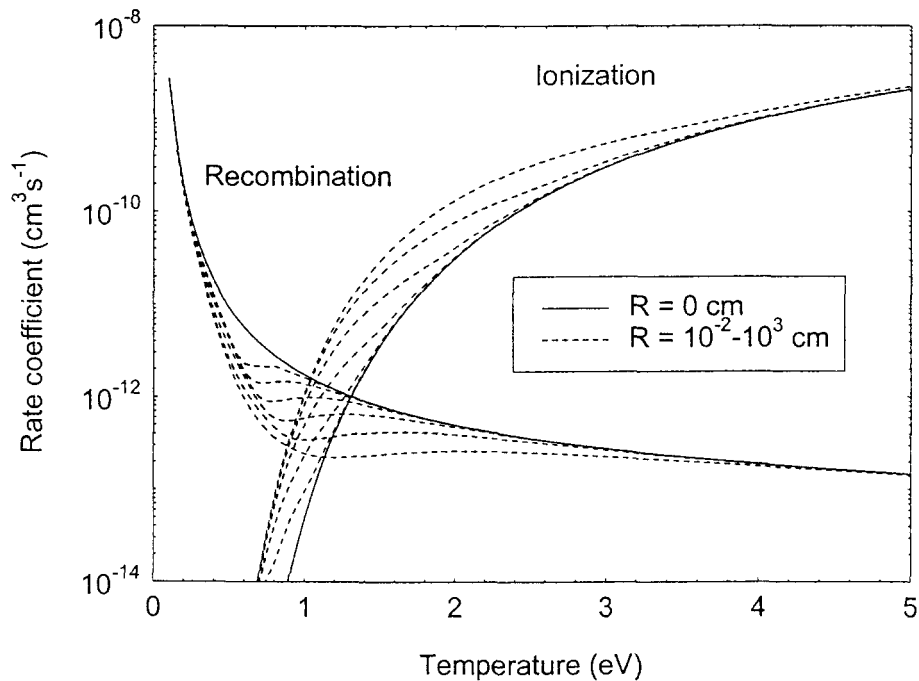
$$R = \int_0^r n_g(r') dr' / n_g(r) \quad (8)$$

where  $n_g$  is the ground state neutral density at position  $r$ , which is measured to the nearest boundary.

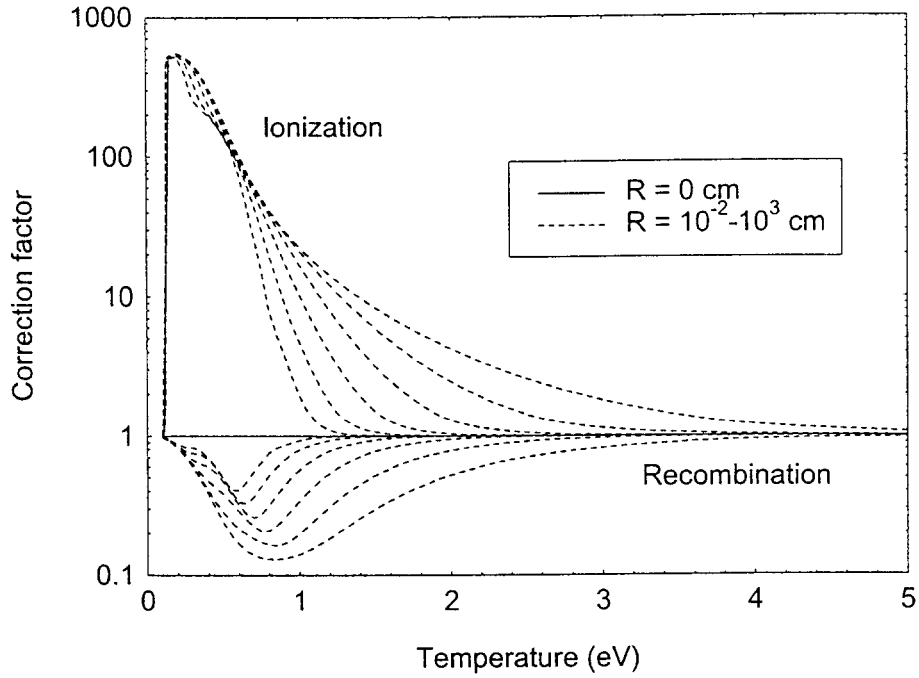
Figure 7 displays the generalized ionization and recombination rate coefficients for an electron density of  $10^{14} \text{ cm}^{-3}$  and a wide range of values of  $R$ . The solid lines ( $R=0$ ) give the optically thin SPR values. For temperatures below 2 eV, radiation effects dramatically change the rates. This is more easily seen in Figure 8, which displays the ratios of the generalization rate coefficients to the optically thin values.

Figure 9 shows the generalization of the tabulated energy changes per transition. The ionization values decrease slightly with increasing optical depth as ionizations occur out of excited states. The recombination values differ dramatically at low temperatures, as recombinations to the ground state are largely balanced by radiative excitations. The limiting case where recombinations only occur to the first excited state ( $E_r=3.4 \text{ eV}$ ) is equivalent to that used by Knoll in his simulations [6,7].

These coefficients were calculated using the radiation field present in the center of a spatially uniform plasma slab of extent  $2R$ , assuming thermally broadened line profiles. The use of thermal broadening at this electron density can be justified by noting that trapping the first few Lyman lines, which have negligible Stark broadening, produces almost all of the change. Zeeman splitting, however, can decrease the optical depth by up to a factor of two, producing a corresponding decrease in the appropriate value of  $R$  for given plasma profiles. Future work will be required to clarify this correspondence, but the expected changes are much smaller than the overall effects of radiation trapping.



**FIGURE 7.** Effective ionization and recombination coefficients as a function of temperature for  $n_e=10^{14} \text{ cm}^{-3}$ . The solid curves are for an optically thin plasma ( $R=0$ ). The dotted curves are for six different optical depths, parameterized by the effective distance  $R$  with values ranging from  $R=10^{-2} \text{ cm}$  to  $R=10^3 \text{ cm}$ . The effective width increases by a factor of 10 for each successive curve.



**FIGURE 8.** Correction factor for the optically-thin effective ionization and recombination rates for the same cases as in Figure 7. The correction factor is defined as the ratio of the rate to the optically-thin value.

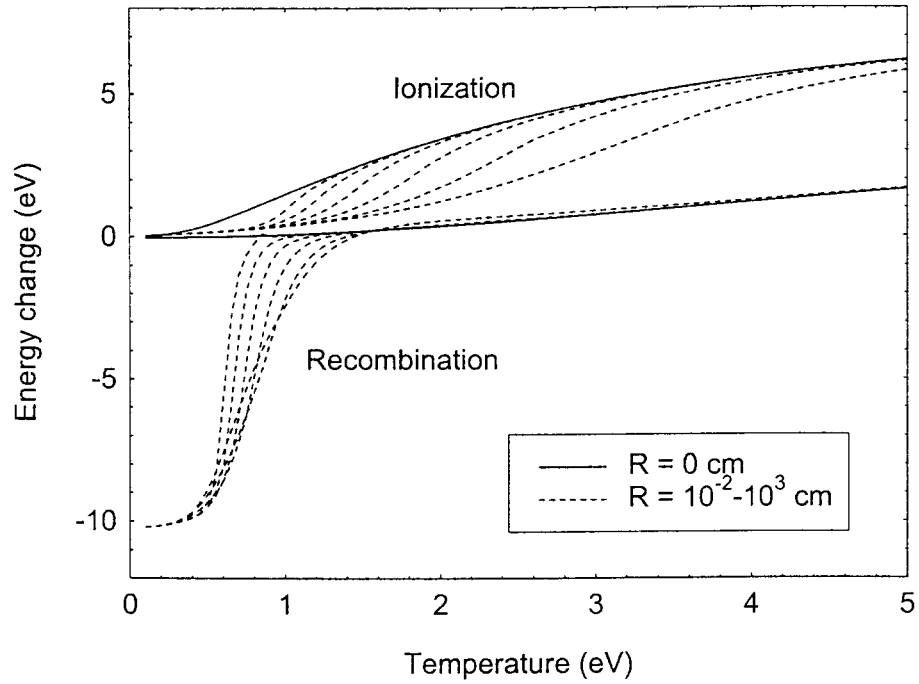


**FIGURE 9.** Average electron energy change per transition for ionization ( $\delta E_z$ ) and recombination ( $\delta E_R$ ) for the same cases as Figure 7.

## DISCUSSION

The first few steps towards incorporating radiation transport in edge plasma simulations are now complete. Line profiles in magnetized plasmas are available from the modified TOTAL code, for complex atoms as well as for hydrogen. The line profiles can be used for diagnostics in optically thin situations [10] and have been integrated into the CRETIN code for accurate calculations of radiation flow in optically thick plasmas.

As a step towards evaluating the effects of line radiation in edge plasmas, tables incorporating the modified SPR coefficients can be used by making minor modifications in existing edge plasma codes, and we have begun experimenting with these in the UEDGE code. We are also constructing a one-dimensional code that combines edge plasma transport processes and radiation transport. This will allow us to validate and improve the tabulated coefficients, as well as investigate other possible integration procedures. We expect these developments to substantially improve our understanding of radiation effects in tokamak edge plasmas.

## ACKNOWLEDGMENTS

We would like to thank R.W. Lee and H.K. Chung (LLNL) for their valuable contributions.

This work was performed under the auspices of the U.S. Department of Energy by the University of California, Lawrence Livermore National Laboratory through contract number W-7405-Eng-48.

## REFERENCES

1. Terry, J. L., Lipschultz, B., Bonnin, X., Boswell, C., Krasheninnikov, S. I., Pigarov, A. Yu., LaBombard, B., Pappas, D., and Scott, H. A., *J. Nucl. Mater.* **266-269**, 30 (1999).
2. Isler, R. C., McKee, G. R., Brooks, N. H., West, W. P., Fenstermacher, M. E., and Wood, R. D., *Phys. Plasma* **4**, 2989 (1997).
3. Terry, J. L., Lipschultz, B., Pigarov, A. Yu., Krasheninnikov, S. I., LaBombard, B., Lumma, D., Ohkawa, H., Pappas, D., and Umansky, M., *Phys. Plasma* **5**, 1759 (1998).
4. Wan A. S., Dalhed H. E., Scott H. A., Post D. E., and Rognlien T. D., *J. Nucl. Mater.* **220-222**, 1102 (1995).
5. Rognlien T. D., Milovich, J. L., Rensink, M. E., and Porter, G. D., *J. Nucl. Mater.* **196-198**, 347 (1992).
6. Knoll, D. A., P. R. McHugh, S. I. Krasheninnikov, and D. J. Sigmar, *Phys. Plasma* **3**, 293 (1996).
7. Knoll, D. A., *Nuclear Fusion* **38**, 133 (1998).
8. A. Calisti, Khelfaoui, F., Stamm, R., Talin, B., and Lee, R. W., *Phys. Rev A*, **42**, 5433 (1990).
9. Scott, H. A., *JQSRT*, **71**, 689 (2001).
10. Adams, M. L., Lee, R. W., Scott, H. A., Chung, H. K., and Klein, L., "Atomic Line Shapes in the Presence of an External Magnetic Field" in *Atomic Processes in Plasmas: 13<sup>th</sup> APS Topical Conference on Atomic Processes in Plasmas*, edited by D. R. Schultz and F. W. Meyer, AIP Conference Proceedings 635, New York: American Institute of Physics, 2002, pp. 261-272.
11. Adams, M. L., Lee, R. W., Scott, H. A., Chung, H. K., and Klein, L., *Phys. Rev E* (in press).
12. Novikov, V. G., Vorob'ev, V. S., D'yachkov, L. G., and Nikiforv, A. F., *JETP* **92**, 441 (2001).
13. Stotler, D. P., Post, D. E., and Reiter, D., *Bul. Am. Phys. Soc.* **38**, 1919 (1993).